ARTICLE

Manganese Complexes with Chelating and Bridging Di-Triazolylidene Ligands: Synthesis and Reactivity

Received 00th January 20xx,
Accepted 00th January 20xx

DOI: 10.1039/x0xx00000x

Sofia Friães,[a] Sara Realista,[a] Clara S. B. Gomes,[b] Paulo N. Martinho,[c] Luís F. Veiros,[d] Martin Albrecht,[e] Beatriz Royo*[a]

New manganese complexes bearing di-triazolylidene (di-trz) ligands are described. Depending on the wingtip substituents of the triazolylidene ligand and the synthetic procedure, two different ligand coordination modes were observed, *i.e*, bridging and chelating. A series of Mn(I) complexes of the general type *fac*-[Mn(di-trz^{R})(CO)$_3$Br] (R = Me, Et, Mes) with a chelating di-trz ligand were prepared via Ag-transmetalation. In contrast, the *in situ* deprotonation of the triazolium salts with KOBu^{t} yielded the bimetallic Mn(0) complexes [Mn$_2$(CO)$_8$(μ-di-trz^{R})] with a bridging di-trz ligand when short alkyl chains (Me, Et, *i*-Pr) are present as the N1 substituents of the triazolylidene ligand. The molecular structures of monometallic and bimetallic complexes were determined by X-ray diffraction studies. In addition, the cationic *fac*-[Mn(di-trz^{Et})(CO)$_2$(PPh$_3$)$_2$]Br complex, a rare example of a dicarbonyl Mn(I) N-heterocyclic carbene, was obtained when *fac*-[Mn(di-trz^{Et})(CO)$_3$Br] was irradiated with visible light in the presence of PPh$_3$. The crystal structure revealed a slightly distorted octahedral geometry around the Mn(I) centre, with the chelating di-triazolylidene ligand situated in *trans* position to the two CO ligands in the equatorial plane, and the two phsophine ligands occupying the axial positions. Cyclic voltammetry studies show reversible redox processes for the monometallic Mn(I) complexes, and a quasi-reversible EC mechanism for the oxidation of the bimetallic complexes. Infrared spectroelectrochemical studies along with DFT calculations for *fac*-[Mn(di-trz^{Et})(CO)$_3$Br] suggest that the observed two consecutive reductions occur both at the metal centre.

Introduction

Triazolylidenes (trz) have developed in recent years as a burgeoning subclass of NHC ligands.[1-5] Their modular synthesis through Cu(I) catalysed click reactions, which allows for tailoring them to specific functions, and their strong sigma-donor properties have made them excellent candidates as carbene ligands for transition metals. To date, triazolylidene metal complexes have been mainly applied in catalysis.[3] However, their potential in other fields such as, photochemistry,[6-9] supramolecular chemistry,[10,11] and electrocatalysis[12] has been recently demonstrated. Most examples of triazolylidene complexes reported in the literature contain second- and third-row transition metals, while the trz chemistry of first-row transition metals remains poorly developed.[13-19] In particular, Mn complexes bearing triazolylidene ligands are very scarce.[20,21]

In line with our interest in N-heterocyclic carbene chemistry of 3d metals,[14,15,22-34] we recently described two rare examples of Mn complexes incorporating di(1,2,3-triazolylidene) (di-trz) ligands (Chart 1).[21] Notably, the only other example of a Mn-triazolylidene complex reported so far is a Mn(0) tricarbonyl complex bearing a 1,2,3-triazolylidene-based tripodal ligand, described by Smith and co-workers in 2013 (Chart 1).[20] In our recent studies, directly linked di-trz ligands were coordinated to Mn by reaction of their di-triazolium salts with Mn(CO)$_5$Br in the presence of KOBu^{t}. When the di-trz ligand contains an ethyl substituent in the N1 positions, the reaction led to a bimetallic Mn(0) complex, in which the ligand adopted a bridging rather than chelating binding mode (Chart 1). In contrast, coordination of di-trz with the bulky mesityl substituents in N1, yielded a manganese complex with chelating di-trz ligand (Chart 1). While the selectivity was remarkable, the origin of the different product formation was unclear. In this work here, we have extended our studies to investigate the influence of the wingtip substituents (Me, *i*-Pr, *n*-Bu, *p*-tolyl) of the di-trz ligand on the product obtained by metalation of the triazolium salts. In addition, we demonstrate that the metalation procedure determines the type of product obtained. Specifically, coordination of di(1,2,3-triazolylidenes) to Mn(CO)$_5$Br via Ag-transmetalation route selectively affords monometallic *fac*-[Mn(di-trz)(CO)$_3$Br] complexes. In contrast, the *in situ* deprotonation of the corresponding triazolium salts with KOBu^{t} yields bimetallic or monometallic Mn complexes or mixtures of the two, depending on the N1 substituents of the di-trz ligand.

[a] *ITQB NOVA, Instituto de Tecnologia Química e Biológica António Xavier, Universidade Nova de Lisboa, Av. da República, 2780-157 Oeiras, Portugal. E-mail: broyo@itqb.unl.pt.*
[b] *LAQV- and UCIBIO-REQUIMTE, Departamento de Química, Faculdade de Ciências e Tecnologia, Universidade Nova de Lisboa, 2829-516 Caparica, Portugal.*
[c] *Biosystems and Integrative Sciences Institute (BioISI), Faculdade de Ciências, Universidade de Lisboa, Campo Grande, Lisboa, 1749-016, Portugal.*
[d] *Centro de Química Estrutural and Departamento de Engenharia Química, Instituto Superior Técnico, Universidade de Lisboa, Av Rovisco Pais, 1049-001 Lisboa, Portugal*
[e] *Department of Chemistry and Biochemistry, University of Bern, Freiestrasse 3, 3012 Bern, Switzerland.*

† Electronic Supplementary Information (ESI) available: Spectroscopic and electrochemical data, crystallographic and DFT details. CCDC 2060440-2060444.For ESI and crystallographic data in CIF see DOI: 10.1039/x0xx00000x

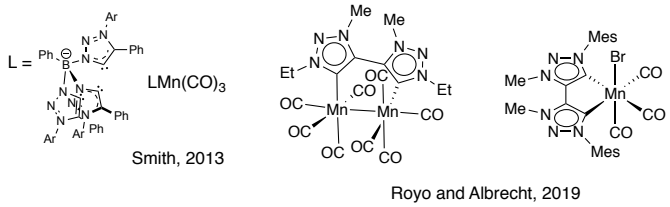

Chart 1 Manganese triazolylidene complexes reported in the literature.

Results and Discussion

Synthesis and Characterisation. The new C4-linked ditriazoles **L1a**, **L1c**, and **L1d** were obtained employing the well-established copper-catalysed click [3+2] cycloaddition reaction that has been previously described for the preparation of **L1b**, **L1e**, and **L1f**.[35,36] Subsequent methylation of the isolated di-triazoles with methyl triflate, followed by anion exchange with tetra-*n*-butylammonium bromide afforded the di-triazolium bromide salts **L2a**-**f** in good yields (Scheme 1). Compounds **L2a**-**f** were characterised by ^{1}H and ^{13}C NMR spectroscopy and HR-MS analysis.

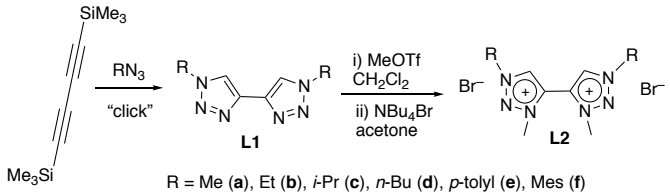

Scheme 1 Synthesis of di-triazolium bromide salts **L2**.

Coordination of proligands **L2a** and **L2c**-**e** to manganese was investigated following the same synthetic approach that was previously reported by us for the coordination of **L2b** (R = Et) and **L2f** (R = Mes).[21] When **L2a** and **L2c**, bearing the Me and *i*-Pr groups on the wingtips, respectively, were treated with $Mn(CO)_5Br$ in the presence of two equivalents of $KOBu^t$, the bimetallic manganese(0) complexes $[Mn_2(CO)_8(\mu\text{-di-trz}^R)]$ [R = Me (**1**) and R = *i*-Pr (**3**)], in which the ligand adopts a bridging binding mode, were isolated as the only products (Scheme 2).

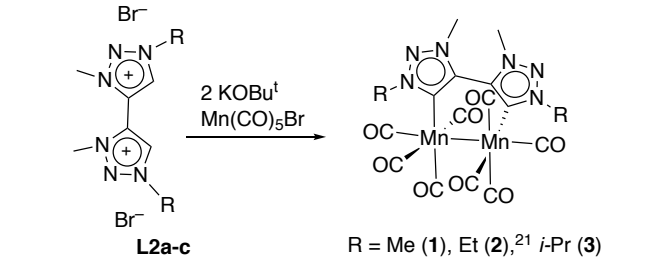

Scheme 2 Synthesis of Mn(0) complexes **1**-**3**.

Complexes **1** and **3** have been fully characterized by NMR and IR spectroscopy, and in the case of **3** by X-ray diffraction studies, Figure 1. Coordination of **L2a** and **L2c** was corroborated by the disappearance of the signals of the triazolium protons at 9.5-9.7 ppm in the ^{1}H NMR spectra, and the appearance of the characteristic resonance of the metalated carbon in the ^{13}C NMR spectra at 181.5 ppm (for **1**) and 180.3 ppm (for **3**). The carbonyl ligands in **1** and **3** showed the expected pattern in the IR spectra, displaying three strong IR bands (in the region 1971-1874 cm^{-1}) and a relatively week band at 2040 cm^{-1} (for **1**) and 2037 cm^{-1} (for **3**), and four resonances at 231, 229, 225, and 223 ppm in their ^{13}C NMR spectra.

In contrast to the results obtained with proligands **L2a**-**L2c**, application of the same synthetic approach for **L2d** and **L2e** afforded a mixture of the corresponding bimetallic and monometallic complexes (Scheme 3). The ratio of bimetallic *vs*. monometallic complexes in these mixtures was 57:43 (for **4**:**6**) and 61:39 (for **5**:**7**) according to ^{1}H NMR spectroscopy (Fig. S25 and S26). These mixtures were difficult to separate, and complexes **4**-**7** could not be isolated in pure form. However, single crystals of **4** and **5** were obtained after several crystallizations and their structures were determined by X-ray diffraction studies (Fig. 1(b) and 1(c), respectively).

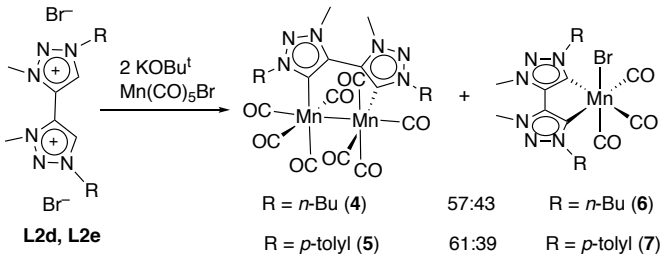

Scheme 3 Synthesis of complexes **4**-**7** from di-triazolium bromide salts **L2d**-**L2e**.

The Mn(0) centres in complexes **3**-**5** display a slightly distorted octahedral geometry, with bond angles close to the expected 90° (Figure 1). In complex **3**, the bond length between the two Mn(0) metal centres (Mn1–Mn2) is 2.9468(10) Å, whereas the Mn1–C1 and Mn2–C7 bond distances are 2.050(4) and 2.051(4) Å, respectively. These values and the remaining bond distances in the molecule are similar to those observed for complexes **4** and **5** (*e.g.* Mn-Mn distances 2.9797(13) Å for **4** and 2.9324(7) Å for **5**). In complex **4**, the dihedral angles between the two triazolylidene rings are 50.96(10)° and 49.5(4)°, for PART 1 and PART 2, respectively, which are very similar to the observed for complex **3** (50.18(17)°). However, in the case of complex **5**, a dihedral angle of 47.36(14)°, closer to that determined for the previously reported complex **2** (46.92(9)°),[21] was observed.

ARTICLE

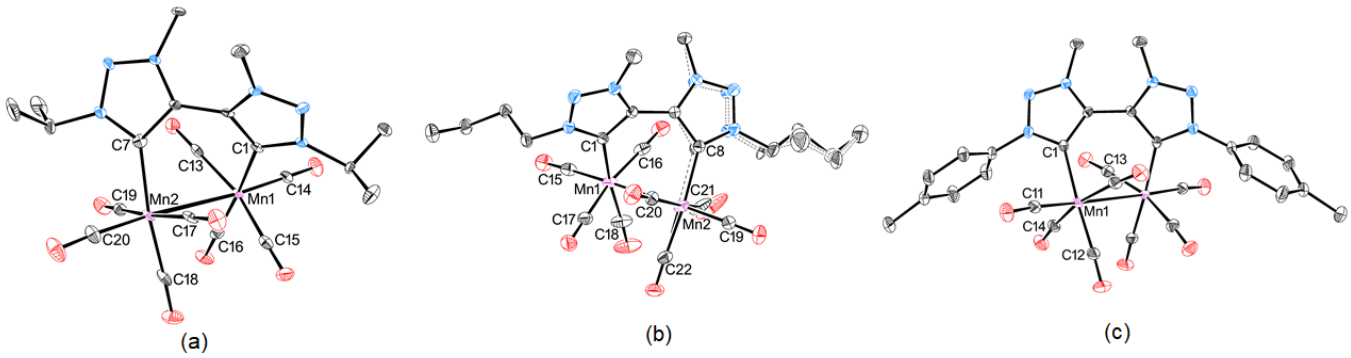

Figure 1 ORTEP-3 diagrams of complexes (a) **3**, (b) **4** and (c) **5** using 50% probability level ellipsoids. All hydrogen atoms were omitted for clarity. In **4**, atoms Mn2, C8, N4, N5, N6, C11, C12 and C13 were found to be disordered over two positions with 80% (PART 1) and 20% (PART 2) probability, depicted in solid and dashed bonds, respectively. In **5**, half molecule was generated by symmetry operations. Selected bond lengths for **3**: Mn1–Mn2 2.9468(10) Å, Mn1–C1 2.050(4) Å, Mn2–C7 2.051(4) Å, Mn1-CO between 1.801(4) and 1.831(4) Å, Mn2-CO between 1.798(5) and 1.854(5) Å. Selected bond lengths for **4**: PART 1 – Mn1–Mn2 2.9797(13) Å, Mn1–C1 2.0443(13) Å, Mn2–C8 2.051(4) Å, Mn1–CO between 1.8000(16) and 1.8518(16) Å, Mn2–CO between 1.752(2) and 1.858(2) Å. Selected bond lengths for **5**: Mn1–Mn1# 2.9324(7) Å, Mn1–C1 2.047(3) Å, Mn1–CO between 1.788(3) and 1.843(3) Å.

These results show that the chelating bonding mode is more preferred when bulkier trz ligands are present (2:3 for R = *p*-tolyl *vs* 1:0 for R = mesityl) However, when the Ag-transmetalation route was applied for the coordination of **L2a**, **L2b**, and **L2f**, the air stable yellow monometallic Mn(I) tricarbonyl complexes containing chelating di-triazolylidene ligands *fac*-[Mn(di-trz^{R})(CO)$_3$Br] [R = Me (**8**), Et (**9**), and Mes (**10**)] were, in all cases, isolated as the only product (Scheme 4).

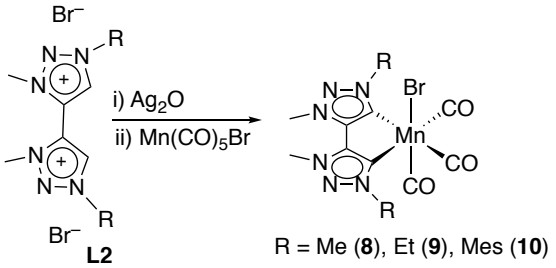

Scheme 4 Synthesis of Mn(I) complexes **8**-**10**.

The identity of complexes **8**-**10** was determined by spectroscopic techniques and elemental analysis. Complex **10** has been previously reported by us.[21] Consistent with the proposed structures, the IR spectra of these complexes displayed the typical patterns for *fac*-carbonyl ligands.[22,23,37] The values of the symmetrical CO stretching vibrations of **8**-**10** appear at lower wavenumbers than those reported for the imidazole-2-ylidene analogue *fac*-[Mn(bis-NHC^{R})(CO)$_3$Br] (2004 cm^{-1} for R = Me, and 2007 cm^{-1} for R = Mes), reflecting the stronger donor capacity of triazolylidenes compared to imidazolylidene ligands.[22,23] Single crystals suitable for X-ray structure analysis were obtained for complex **10** (Fig. 2).

Complex **10** features a slightly distorted octahedral Mn(I) centre with bond angles in the coordination sphere very close to 90°. The chelating di-triazolylidene ligand displays a C1–Mn–C13A bite angle of 77.4(2)°. The Mn–Br bond length is 2.5568(11) Å and the Mn–C$_{CO}$ distances vary between 1.774(7) and 1.833(6) Å, similar to the Mn(0)–CO bond lengths. Likewise, the Mn–C$_{trz}$ bond lengths (2.038(6) and 2.048(6) are essentially identical to those observed in the bridging coordination mode to Mn(0). The dihedral angle between the two triazolylidene rings is 7.4(2)°, which reflects an essentially planar backbone of the ligand as expected for a chelating bonding mode of this ligand.

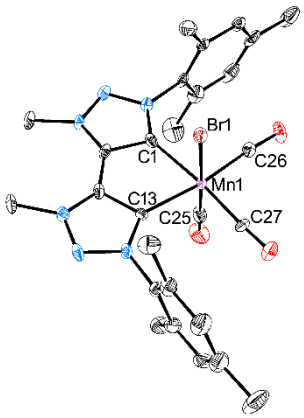

Figure 2 ORTEP-3 diagram of complex **10**, using 50% probability level ellipsoids. All hydrogen atoms, two dichloromethane molecules and a second [Mn(CO)$_3$(di-trz^{Mes})Br] complex were omitted for clarity. Selected bond lengths: Mn1–Br1 2.5568(11) Å, Mn1–C1 2.038(6) Å, Mn1–C13 2.048(6) Å, Mn1–CO between 1.774(7) and 1.833(6) Å.

Interestingly, the reaction of the dimetallic Mn(0) complex **2** with Br$_2$ led to the monometallic complex **9** with the concomitant formation of Mn(CO)$_5$Br, suggesting facile Mn-C$_{trz}$ and Mn-CO bond making and

breaking (Scheme 5). Similar reaction with H_2 did not allow the isolation of the corresponding hydride species.

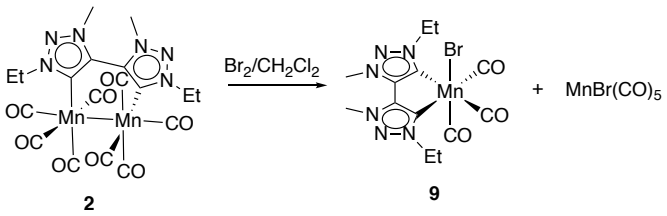

2 **9**

Scheme 5 Reaction of **2** with bromine.

All complexes **1**-**10** are air and moisture stable. They can be stored in the dark under air atmosphere during weeks without any notable decomposition. The thermal stability of complexes **2** and **9** was analysed by thermogravimetric analysis. Complex **2** starts to decompose around 164 °C with 58% weight loss up to 300 °C, which may suggest the loss of the $Mn_2(CO)_8$ fragment (58.9%; Fig. S33). Complex **9** is slightly less stable than **2**, starting to decompose at 146 °C (Fig. S34). In contrast to complex **2**, complex **9** shows two distinct steps, a sharper 25% weight loss in the 146–210 °C temperature ranges, and a more gradual further 25% loss up to about 400 °C, commensurate with an initial dissociation of bromide and one CO, followed by loss of a $Mn(CO)_2$ fragment. For both complexes, the minor weight loss up to *ca*. 150 °C may be due to the loss of residual solvent molecules.

In addition, we were interested in investigating the photochemical stability of **2** and **9**. We observed the loss of carbonyl ligands when acetonitrile solutions of **2** and **9** were exposed to visible light irradiation for several hours (LED, *ca*. 415 nm, 6 h). However, the identification of the products obtained in these decarbonylating reactions was not possible. Interestingly, when the irradiation of acetonitrile solutions of **9** was performed in the presence of two equivalents of PPh_3, the cationic dicarbonyl [Mn(di-trz^{Et})$(CO)_2(PPh_3)_2$]Br (**11**) complex was isolated as a pure compound (Scheme 6). Complex **11** has been fully characterised including the determination of its molecular structure by X-ray diffraction studies. As shown in Figure 3, it features a *trans* arrangement of the NHC and the carbonyl ligands in an octahedral geometry where the PPh_3 ligands are located mutually *trans* and occupying the axial positions. As expected for this type of geometry, the IR spectrum of **11** showed two strong resonances at 1916 and 1834 cm^{-1} for the symmetric and asymmetric CO vibrations, respectively, while the ^{31}P NMR spectrum features one single resonance at δ 69.2 ppm for the two identical phosphorus atoms. The ^{13}C NMR spectrum of **11** displays a resonance of the C_{trz} atom at δ 196.3 ppm, and one resonance at δ 230.9 ppm for the two symmetry-related carbonyl ligands. Complex **11** represents a rare example of a Mn(I) dicarbonyl NHC complex. To the best of our knowledge, the only other example reported in the literature corresponds to a Mn complex containing a NH,NH-substituted saturated cyclic diaminocarbene with a bidentate diphosphine ligand occupying one *cis* and one *trans* position to the NHC donor.[38]

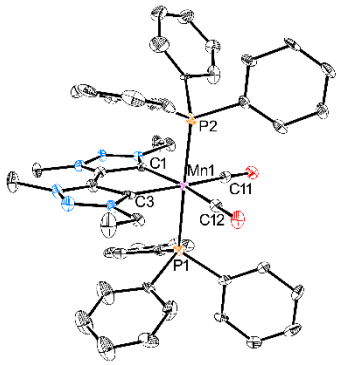

Figure 3 ORTEP-3 diagram of complex **11**, using 30% probability level ellipsoids. All hydrogen atoms, the Br^- counter ion, one acetonitrile and a water molecule were omitted for clarity. Selected bond lengths: Mn1–P1 2.275(3) Å, Mn1–P2 2.287(3) Å, Mn1–C1 2.065(10) Å, Mn1–C3 2.032(10) Å, Mn1–C11 1.758(11) Å, Mn1–C12 1.790(11) Å.

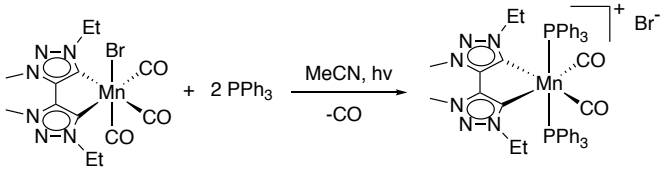

9 **11**

Scheme 6 Reaction of **9** with two equivalents of PPh_3 under visible light (LED, *ca.* 415 nm) irradiation.

When **9** is irradiated in the presence of only one equivalent of PPh_3, we observed the formation of complex **11** that precipitated from the acetonitrile solution, along with the formation of two new Mn complexes that remained in the solution. The ^{31}P NMR of the acetonitrile solution showed one major peak at δ 73.25 ppm, a peak at δ 69 ppm, which corresponds to **11**, and a peak at δ 55 ppm, in a ratio 1:0.3:0.2, respectively (Fig. S40a). The peak at δ 55 ppm was assigned to the Mn(0) dimer species $[Mn_2(CO)_8(PPh_3)_2]$.[39] We propose that the peak at δ 73.25 ppm observed in the ^{31}P NMR corresponds to the cationic tricarbonyl mono phosphine *fac*-[Mn(di-trz^{Et})$(CO)_3(PPh_3)$]Br (**12**) complex (Scheme 7). This proposal is based on the information obtained from the ^{13}C NMR spectrum of the mixture, which showed the expected resonances for a tricarbonyl Mn complex, two resonances at δ 223 and 219 ppm for the carbonyl groups, and one resonance for the carbene at δ 187 ppm (Fig. S40b). Unfortunately, **12** could not be isolated in pure form from the reaction mixture.

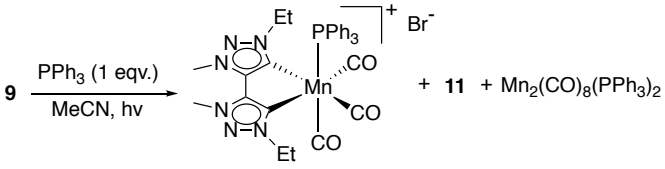

Scheme 7 Reaction of **9** with one equivalent of PPh_3 under visible light (LED, *ca.* 415 nm) irradiation.

Irradiation of the dimetallic complex **2** with visible light (LED, *ca*. 415 nm) in the presence of two equivalents of PPh_3 afforded a mixture of Mn complexes **11**, **12**, $[Mn_2(CO)_8(PPh_3)_2]$, along with a new Mn species of unknown identity that displayed a resonance at δ_P 92.76 ppm (Fig. S41).

Cyclic voltammetry, infrared spectroelectrochemistry and DFT Calculations. As previously found for the bimetallic Mn(0) complex **2**,[21] both **1** and **3** also exhibited one quasi-reversible oxidation process at $E_{1/2}$ = -0.05 and -0.06 V (potential *vs* Fc/Fc^+), respectively, and their responses are indicative of electron-transfer followed by a chemical reaction (EC) mechanism (Table S1 and S2 and Fig. S42). Complexes **9** and **10** showed a reversible oxidation process at $E_{1/2}$ ≈ 0.3 V (Figure 4), shifted to higher potential in comparison with the bimetallic Mn(0) counterparts.[21] The mixtures of **4** and **6**, and those of **5** and **7** showed two oxidation events around -0.05 and +0.3 V, supporting the presence of a mixture of di-Mn(0) and monometallic Mn(I) complexes as deduced by NMR spectroscopy (Fig. S44). In addition to the oxidation processes, the CV of **9** and **10** showed two irreversible one-electron reduction events at $E_{1/2}$ = -2.18 and -2.45 V (for **9**) and $E_{1/2}$ = -2.11 and -2.74 V (for **10**) (Fig. 4). As expected, the cathodic wave of **9** ($E_{1/2}$ = -2.18 V) is negatively shifted when compared to that of **10** ($E_{1/2}$ = -2.11 V), reflecting the stronger donor capacity of the triazolylidene ligand bearing an ethyl group in the N1 position *vs* a mesityl.

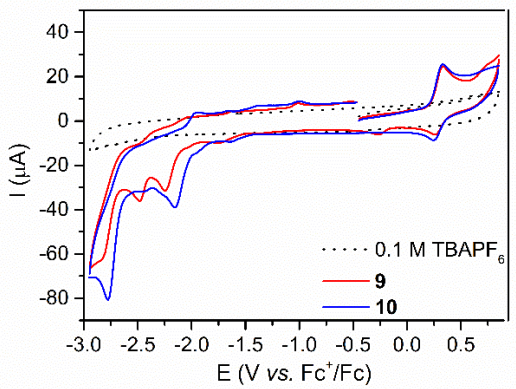

Figure 4 Cyclic voltammograms of complexes **9** and **10** (1mM) in CH_3CN, N_2 saturated solutions using $TBAPF_6$ as supporting electrolyte (0.1 M) at 0.1 V s^{-1}. Glassy carbon (3 mm diameter) was used as working, platinum wire as counter and 3M Ag/AgCl as reference electrodes.

To gain insight into the species formed in the reduction process, the reduction behaviour of **9** was further investigated by infrared spectroelectrochemistry (FTIR-SEC). Experiments performed in acetonitrile, show that the redox events involve a $2e^-$ reduction of **9** to generate the five coordinated anion $[Mn(CO)_3(di\text{-}trz)]$ **[9']**$^-$ with a trigonal bipyramidal geometry (Fig. S51), after the loss of the axial Br^- (Scheme 8). The formation of **[9']**$^-$ is in agreement with DFT calculations and previous studies.[22] In fact, upon the first reduction event, the FTIR-SEC spectra showed the depletion of the ν(CO) bands of the parent complexes (**9** and **9CH$_3$CN**$^+$) with new bands growing at 1943, 1886 cm^{-1}, which can be assigned to the reduced species **9´** (Fig. 5). This assignment is based on the good correlation between the experimental and the DFT-calculated IR spectrum of **9´** (Table 1). The second reduction shows the appearance of new bands that reasonably agree with the calculated CO stretching frequencies for **[9']**$^-$ (Fig. S49, Table 1). DFT calculations suggest that both reduction events occur mainly in the metal centre, as shown by a spin density located at the Mn-atom in the resulting spin doublet intermediate with a square pyramidal geometry, **9'**, and the spin singlet intermediate, **[9']**$^-$, with a trigonal bipyramidal geometry (Fig. S50 and S51, respectively)

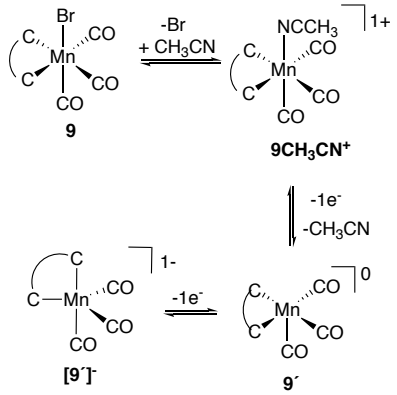

Scheme 8 Proposed species formed in the $2e^-$ reduction of **9** in acetonitrile.

Table 1 Experimental and DFT calculated harmonic vibrational frequencies for the highest CO stretching frequency.[a]

Species	Experimental ν_{CO} (cm^{-1})	Calculated ν_{CO} (cm^{-1})
9	1999	2000
9CH$_3$CN$^+$	2019	2022
9´	1943	1940
[9´]$^-$	1844	1855

[a]Details can be found in the SI.

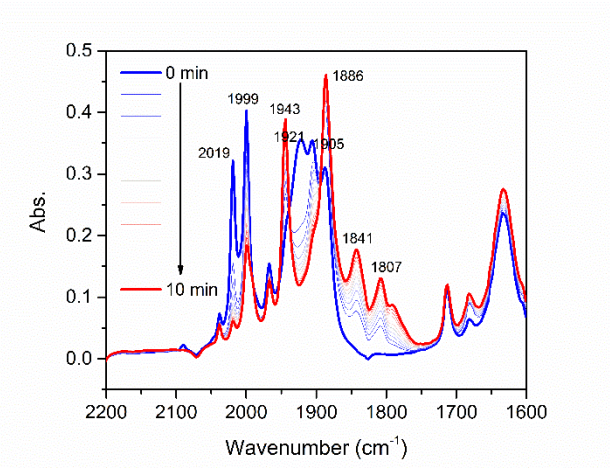

Figure 5 FTIR-SEC experiments during the first reduction (at *ca.* -2.1 V) using 5 mM of **9** and 0.1 M $TBAPF_6$ in a N_2 saturated CH_3CN solution, Pt grids as working and counter electrodes and Ag wire as pseudo-reference electrodes. Blue spectrum corresponds to 0 min and red corresponds to the spectrum recorded after 10 min of experiment.

Conclusions

Here we demonstrate the versatility of di-triazolylidene ligands to stabilize both bimetallic Mn(0) as well as monometallic Mn(I) complexes. Depending on the applied synthetic procedure and

the steric demand of the triazole wingtip groups, this ditopic ligand assumes either a bridging coordination mode to two Mn(0) centres, or a chelating bonding mode to a single Mn(I) centre. A facile oxidation strategy using bromine allows to convert the bridging into the chelating bonding mode. Further functionalization provided access to [Mn(di-trz^{Et})(CO)$_2$(PPh$_3$)$_2$]Br, a rare example of a Mn dicarbonyl NHC complex and demonstrates the potential for ligand substitution and tailoring of the properties of the Mn(di-trz) unit. Moreover, electrochemical reduction suggests the formation of a coordinatively unsaturated Mn(0) complex with a free coordination site, which provides ample opportunities for substrate binding. Evaluation of the (electro)catalytic activity of these complexes is currently under investigation in our laboratories.

Experimental details

General methods

All reactions and manipulations were carried out under nitrogen atmosphere using standard Schlenk techniques, and solvents were purified from appropriate drying agents. Deuterated solvents were degassed and stored over molecular sieves. All other reagents were purchased from commercial suppliers and used without further purification. Preparation of compounds **L1b**, **L1f**, **L2b**, **L2f** were performed following the procedure reported in the literature.[35,36] Complex **2** was prepared according to literature procedure.[21] ^{1}H and ^{13}C NMR spectra were recorded on a Bruker Avance III 400 MHz and Bruker Avance II 500 MHz. Electrospray mass spectra (ESI-MS) were recorded on a Micromass Quatro LC instrument; nitrogen was employed as drying and nebulising gas. Elemental analyses were performed in our ITQB laboratory services. TGA analyses were performed in TGA Q50 V6.7 Build 203 instrument, with 9-12 mg sample in an aluminium pan, over a temperature range of 25-500 °C, under nitrogen atmosphere at a heating rate of 5 °C/min.

General procedure for the synthesis of L1a, **c**, and **d.**

A mixture of RI (R = Me, *i*-Pr, *n*-Bu) (4.49 mmol) and NaN_3 (875 mg, 13.50 mmol) in THF/H_2O (30 mL, 1:1 v/v) was stirred at room temperature for 16 h. Then, 1,4-bis(trimethyl)silylbutadiyne (411 mg, 2.10 mmol), pyridine (0.298 ml, 3.70 mmol), K_2CO_3 (582 mg, 4.20 mmol), $CuSO_4$ (73 mg, 0.46 mmol), and Na-ascorbate (589 mg, 3.00 mmol), were added, and the reaction mixture was refluxed for 48 h. After cooling to room temperature, the solvent was removed under vacuum, and the residue was extracted with CH_2Cl_2 (3 x 50 mL). The combined organic layers were washed with 10% ammonium hydroxide solution (2 x 50 mL), water (2 x 50 mL) and brine (2 x 50 mL), dried over Na_2SO_4, and filtered. All volatiles were removed from the filtrate under reduced pressure to yield the corresponding ditriazoles **L1a**, **L1c**, and **L1d** as white solids.

Characterisation of L1a: (39%, 134 mg). ^{1}H NMR (400 MHz, DMSO-d$_6$, 298 K) δ = 8.41 (s, 2H, H$_{trz}$), 4.09 (s, 6H, NC$\underline{H}_3$). ^{13}C{^{1}H} NMR (100 MHz, DMSO-d$_6$, 298 K): δ = 139.17 ($\underline{C}_{trz}$-NCH$_3$), 122.38 ($\underline{C}_{trz}$-H), 36.38 (N$\underline{C}$H3).

Characterisation of L1c: (59%, 273 mg). ^{1}H NMR (400 MHz, DMSO-d$_6$, 298 K): δ 8.53 (s, 2H, H$_{trz}$), 4.90-4.84 (m, 2H, NC$\underline{H}$(CH$_3$)$_2$), 1.54 (s, 6H, NCH(C$\underline{H}_3$)$_2$), 1.52 (s, 6H, NCH(C$\underline{H}_3$)$_2$). ^{13}C{^{1}H} NMR (100 MHz, DMSO-d$_6$, 298 K): δ 139.18 ($\underline{C}_{trz}$-NCH(CH$_3$)$_2$), 119.45 ($\underline{C}_{trz}$-H), 52.52 (N$\underline{C}$H(CH$_3$)$_2$), 22.59 (NCH($\underline{C}$H$_3$)$_2$).

Characterisation of L1d: (79%, 412 mg). ^{1}H NMR (400 MHz, CDCl$_3$, 298 K): δ 8.03 (s, 2H, H$_{trz}$), 4.41 (t, *J* = 7.16 Hz, 4H, NC$\underline{H}_2$CH$_2$CH$_2$CH$_3$), 1.96-1.88 (m, 4H, NCH$_2$C$\underline{H}_2$CH$_2$CH$_3$), 1.42-1.33 (m, 4H, NCH$_2$CH$_2$C$\underline{H}_2$CH$_3$), 0.93 (t, *J* = 7.42 Hz, 6H, NCH$_2$CH$_2$CH$_2$C$\underline{H}_3$). ^{13}C{^{1}H} NMR (100 MHz, CDCl$_3$, 298 K): δ 140.31 ($\underline{C}_{trz}$-H), 120.46 ($\underline{C}_{trz}$-NCH$_2$CH$_2$CH$_2$CH$_3$), 50.32 (N$\underline{C}$H$_2$CH$_2$CH$_2$CH$_3$), 32.32 (NCH$_2$$\underline{C}H_2CH_2CH_3$), 19.77 (NCH$_2CH_2$$\underline{C}H_2CH_3$), 13.55 (NCH$_2CH_2CH_2$$\underline{C}H_3$).

General procedure for the preparation of L2a-f.

The appropriate ditriazole **L1** (1.98 mmol) was dissolved in the minimum quantity of dichloromethane, and MeOTf (0.87 mL, 7.92 mmol) was added at 0 °C. The mixture was stirred at room temperature for 48 h. Then, diethyl ether was added to the mixture to yield a white precipitate that was collected by filtration, dried in vacuum, redissolved in a minimum amount of acetone, and treated with tetra-*n*-butyl ammonium bromide (996 mg, 3.09 mmol). After stirring for 10 min, a white solid precipitated from the solution. The solid was isolated by filtration, washed with acetone and ether, and dried under vacuum to yield the corresponding di-triazolium bromide salts **L2a**-**L2f**, as white solids.

Characterisation of L2a: (88%, 616 mg). ^{1}H NMR (400 MHz, DMSO-d$_6$, 298 K): δ 9.45 (s, 2H, H$_{trz}$), 4.47 (s, 6H, NCH_3), 4.34 (s, 6H, NCH_3). ^{13}C{^{1}H} NMR (100 MHz, DMSO-d$_6$, 298 K): δ 133.89 (C_{trz}-NCH$_3$), 126.42 ($\underline{C}_{trz}$-H), 40.60 (NCH$_3$). ESI-HRMS *m/z* [M-2Br]$^{2+}$ 97.0633, calc 97.0640.

Characterisation of L2b: (65%, 493mg). ^{1}H NMR (400 MHz, DMSO-d$_6$, 298 K): δ = 9.68 (s, 2H, H$_{trz}$), 4.83 (q, *J* = 7.28 Hz, 4H, NCH_2CH$_3$), 4.41 (s, 6H, NCH_3), 1.62 (t, *J* = 7.29 Hz, 6H, NCH$_2$CH_3). ^{13}C{^{1}H} NMR (100 MHz, DMSO-d$_6$, 298 K) δ 132.67 (C_{trz}-H), 126.58 (C_{trz}-NCH$_3$), 49.59 (NCH$_2$CH$_3$), 14.16 (NCH$_2$$CH_3$). ESI-HRMS *m/z* [M-2Br+MeO]$^+$ 253.1762, calc 253.1777.

Characterisation of L2c: (78%, 631 mg). ^{1}H NMR (400 MHz, DMSO-d$_6$, 298 K): δ 9.70 (s, 2H, H$_{trz}$), 5.30-5.23 (m, 2H, NCH(CH$_3$)$_2$), 4.42 (s, 6H, NCH_3), 1.68 (d, *J* = 6.67 Hz, 12H, NCH(CH_3)$_2$). ^{13}C{^{1}H} NMR (100 MHz, DMSO-d$_6$, 298 K): δ 131.46 (C_{trz}-NCH(CH$_3$)$_2$), 126.74 (C_{trz}-H), 58.44 (NCH(CH$_3$)$_2$), 39.66 (NCH$_3$), 21.73 (NCH(CH$_3$)$_2$). ESI-HRMS *m/z* [M-Br]$^+$ 329.10768, calc 329.10893; [M-2Br]$^{2+}$ 125.09459, calc 125.09529.

Characterisation of L2d: (73%, 635 mg). ^{1}H NMR (400 MHz, DMSO-d$_6$, 298 K): δ 9.54 (s, 2H, H$_{trz}$), 4.79 (t, *J* = 7.04 Hz, 4H, NCH_2CH$_2$CH$_2$CH$_3$), 4.36 (s, 6H, NCH$_3$), 2.02-1.93 (m, 4H, NCH$_2$CH_2CH$_2$CH$_3$), 1.43-1.34 (m, 4H, NCH$_2$CH$_2$CH_2CH$_3$), 0.95 (t, *J* = 7.37 Hz, 6H, NCH$_2$CH$_2$CH$_2$CH_3). ^{13}C{^{1}H} NMR (100 MHz, DMSO-d$_6$, 298 K): δ 132.80 (C_{trz}-H), 126.78 (C_{trz}-NCH$_2$CH$_2$CH$_2$CH$_3$), 53.63 (NCH$_2$CH$_2$CH$_2$CH$_3$), 30.67 (NCH$_2$$CH_2CH_2CH_3$), 18.66 (NCH$_2CH_2$$CH_2CH_3$), 13.23 (NCH$_2CH_2CH_2$$CH_3$).

ESI-HRMS *m/z* [M-Br]$^+$ 359.13692, calc 359.13818; [M-2Br]$^{2+}$ 139.11026, calc 139.11094.

Characterisation of L2e: (84%, 840 mg). ^{1}H NMR (400 MHz, DMSO-d_6, 298 K): δ 10.37 (s, 2H, H_{trz}), 8.05 (d, *J* = 8.39 Hz, 4H, C*H*-*p*-tolyl), 7.65 (d, *J* = 8.32 Hz, 4H, C*H*-*p*-tolyl), 4.65 (s, 6H, NCH_3), 2.48 (s, 6H, CH_3-*p*-tolyl). ^{13}C NMR (100 MHz, DMSO-d_6, 298 K): δ 142.66, 132.29, 131.03 (C_{trz}-H), 130.90 (*C*H-*p*-tolyl), 127.39, 121.66 (*C*H-*p*-tolyl), 20.84 (CH_3-*p*-tolyl). ESI-HRMS *m/z* $[M-2Br]^{2+}$ 173.0942, calc 173.0953.

Characterisation of L2f: (83%, 922 mg). ^{1}H NMR (400 MHz, DMSO-d_6, 298 K): δ 10.12 (s, 2H, H_{trz}), 7.29 (s, 4H, C*H*-Mes), 4.63 (s, 6H, NCH_3), 2.40 (s, 6H, CH_3-Mes), 2.16 (s, 12H, CH_3-Mes). ^{13}C NMR (100 MHz, DMSO-d_6, 298 K): δ 142.41, 134.53 (C_{trz}-H), 134.31, 130.86, 129.64 (C*H*-Mes), 128.37, 40.59 (N*C*H_3), 20.75 (*C*H_3-Mes), 16.93 (*C*H_3-Mes). ESI-HRMS *m/z* $[M-2Br]^{2+}$ 201.1252, calc 201.1266.

General procedure for the synthesis of complexes 1 and 3.
Solid $Mn(CO)_5Br$ (175 mg, 0.64 mmol) was suspended in THF (20 mL) and potassium *tert*-butoxide (124 mg, 1.11 mmol) was added first, followed by addition of the ditriazolium bromide salt (0.5 mmol) at 60 °C. The resulting suspension was heated to 60 °C for 16 h under stirring. All volatiles were removed under vacuum, the residue was washed with Et_2O (3 x 15 mL) and re-dissolved in CH_2Cl_2 (80 mL). The CH_2Cl_2 solution was then washed with water (80 mL) and the organic extract dried with Na_2SO_4. The solution was filtered and concentrated to dryness under vacuum to yield complexes **1** and **3**, which were isolated as orange solids.

Characterisation of 1. (35%, 59 mg). ^{1}H NMR (400 MHz, DMSO-d_6, 298 K): δ 4.35 (s, 6H, NCH_3), 4.14 (s, 6H, NCH_3). ^{13}C NMR (125 MHz, DMSO-d_6, 298 K): δ 231.34 (*C*O), 229.37 (*C*O), 225.29 (*C*O), 223.60 (*C*O), 181.52 (C_{trz}), 138.52 (C_{trz}-NCH$_3$), 40.77 (N*C*H$_3$), 38.33 (NC*H*$_3$). IR (KBr, cm^{-1}): 2040 (vs), 1971 (vs), 1943 (vs), 1924 (vs), 1885 (vs).

Characterisation of 3. (32%, 50 mg). ^{1}H NMR (400 MHz, DMSO-d_6, 298 K): δ 5.56-5.49 (m, 2H, NC*H*(CH$_3$)$_2$), 4.17 (s, 6H, NCH_3), 1.71 (d, *J* = 6.65 Hz, 6H, NCH(CH_3)$_2$), 1.57 (d, *J* = 6.58 Hz, 6H, NCH(CH_3)$_2$). ^{13}C NMR (125 MHz, DMSO-d_6, 298 K): δ 231.17 (*C*O), 229.27 (*C*O), 225.31 (*C*O), 222.99 (*C*O), 180.28 (C_{trz}), 137.47 (C_{trz}-NCH(CH$_3$)$_2$), 56.65 (N*C*H(CH$_3$)$_2$), 38.77 (NCH$_3$), 23.44 (NCH(CH$_3$)$_2$), 22.34 (NCH(CH$_3$)$_2$). IR (KBr, cm^{-1}): 2037 (m), 1970 (s), 1931 (vs), 1912 (vs), 1881 (s). Elem. anal. calcd for $C_{20}H_{20}Mn_2N_6O_8$: C 41.25; H 3.46; N 14.43%. Found: C 41.03; H 3.65; N 14.12%.

General procedure for the synthesis of complexes [(di-trz)Mn(CO)$_3$Br] 8 and **9**. The appropriate di-triazolium bromide salt was dissolved in dry dichloromethane, Ag_2O (1 mmol) was added at room temperature, and the mixture was stirred for 24 h. Then, $Mn(CO)_5Br$ (1 mmol) was added, and the mixture was heated at 50 °C for 72 h. After cooling to room temperature, the solution was filtered through a pad of celite, and concentrated to dryness. The residue was washed with Et_2O (3 x 15 mL), redissolved in CH_2Cl_2 (80 mL), and the solution was washed with water (80 mL). The organic phase was dried with Na_2SO_4, filtered, and the solvent removed under vacuum to yield the desired complex isolated as a yellow solid.

Characterisation of 8: (75%, 105 mg). ^{1}H NMR (400 MHz, DMSO-d_6, 298 K): δ 4.54 (s, 6H, NCH$_3$), 4.33 (s, 6H, NCH$_3$). ^{13}C NMR (125 MHz, DMSO-d_6, 298 K): δ 218.83 (*C*O), 218.46 (*C*O), 182.19 (C_{trz}), 141.66 (N*C*H$_3$). IR (KBr, cm^{-1}): 1999 (vs), 1885 (vs). Elem. anal. calcd. for $C_{11}H_{12}BrMnN_6O_3$: C 32.14; H 2.94; N 20.44%. Found: C 31.91; H 2.64; N 20.83%.

Characterisation of 9: (46%, 102 mg). ^{1}H NMR (400 MHz, DMSO-d_6, 298 K): δ 4.66 (q, 4H, NCH_2CH$_3$), 4.54 (s, 6H, NCH_3), 1.58 (t, *J* = 7.2 Hz, 6H, NCH$_2$CH_3). ^{13}C NMR (125 MHz, DMSO-d_6, 298 K): δ 219.00 (*C*O), 218.72 (*C*O), 180.91 (C_{trz}), 141.61(C_{trz}-NCH$_2$CH$_3$), 48.32 (N*C*H$_2$CH$_3$), 15.41 (NCH$_2$*C*H$_3$). IR (KBr cm^{-1}): 1996 (vs), 1899 (vs), 1883 (vs). Elem. anal. calcd. for $C_{13}H_{16}BrMnN_6O_3$: C 35.56; H 3.67; N 19.14%. Found: C 35.22; H 3.33; N 18.91%.

Synthesis of 9 from complex 2: Complex **2** (96 mg, 0.17 mmol) was dissolved in the minimum quantity of dichloromethane and bromine (2 eq.) was added to the sample. The mixture was stirred for 2h, and then, all volatiles were removed under vacuum. The residue was extracted in a mixture of dichloromethane and water. The organic phase was dried with Na_2SO_4, filtered, and the solvent was removed under vacuum to yield **9** as a yellow solid (99%, 74 mg).

Synthesis of complex 10. The ditriazolium bromide salt **L2f** (112 mg, 0.2 mmol), Ag_2O (162 mg, 0.7 mmol) and KBr (238 mg, 2 mmol) were suspended in dry acetonitrile (10 mL), and the mixture was stirred under exclusion from light for 2 days at 50 °C. Then, the solution was filtered through a pad of celite and the filtrate evaporated to dryness. The crude obtained was redissolved in dry tetrahydrofuran (15 mL), $Mn(CO)_5Br$ (27 mg, 0.1 mmol) was added, and the mixture was stirred at 60 °C for 2 days. The solution was then filtered through a pad of celite and evaporated to dryness. The residue was washed with Et_2O (3 x 15 mL), and redissolved in CH_2Cl_2 (80 mL). The CH_2Cl_2 solution was washed with water (80 mL) and the organic phase dried with Na_2SO_4. (40%, 25 mg). ^{1}H NMR, IR spectroscopy and elemental analysis data were in accord with previously data reported for complex **10**.[21] Single crystals of **10** were obtained by crystallization with CH_2Cl_2/Et_2O.

Synthesis of [Mn(di-trz^{Et})(CO)$_2$(PPh$_3$)$_2$]Br (11) A 5 mL Schlenk tube was charged with complex **9** (22.4 mg, 0.05 mmol), two equivalents of PPh_3 (32 mg, 0.13 mmol), and acetonitrile (2 mL). The mixture was stirred at room temperature and irradiated with violet LEDs (*ca.*415 nm, 9.5 W) for 8h. Then, a precipitate was formed, which was isolated by filtration, washed with diethyl ether and dried under vacuum to yield **11** as a yellow solid. (25%, 12 mg). ^{1}H NMR (400 MHz, CD_2Cl_2, 298 K): δ 7.27 (s, 30H, C*H*-PPh$_3$), 4.71 (s, 6H, NCH_3), 3.18 (q, 4H, NCH_2CH$_3$), 0.90 (t, *J* = 6.90 Hz, 6H, NCH$_2$CH_3). ^{13}C NMR (125 MHz, CD_2Cl_2, 298 K): δ 230.87 (*C*O), 196.31 (C_{trz}), 139.77, 138.08, 137.94, 137.81, 134.20, 134.06, 133.32, 129.61, 128.94, 128.39, 47.90 (N*C*H$_2$CH$_3$), 41.31 (N*C*H$_3$), 12.64 (NCH$_2$*C*H$_3$). ^{31}P NMR (400 MHz, CD_2Cl_2, 298 K): δ 69.23. IR (KBr, cm^{-1}): 1916 (s), 1834 (vs). HRMS *m/z* $[M-Br]^+$ 855.2526, calc 855.2524.

Electrochemical studies. Cyclic voltammetry experiments were performed in a three-electrode one compartment electrochemical using glassy carbon (CHI Instruments, 3 mm diameter) and platinum wire were used as working and counter electrodes, respectively. Ag/AgCl 3M KCl electrode (CHI Instruments) was used as reference electrode and tetrabutylammonium hexafluorophosphate ($TBAPF_6$) as supporting electrolyte (recrystallised from hot ethanol). All

potentials are referenced to ferrocene/ferrocenium couple. The working electrode was polished with alumina pastes of 1 and 0.05 µm diameter sizes and washed thoroughly with Milli-Q water and dried under a nitrogen flux. All complexes **1-10** were studied in CH_3CN solutions whereas complex **11** was studied in CH_2Cl_2 solution. The cyclic voltammograms were recorded using a Bioanalytical Systems CV-50W Voltammetric Analyzer (BASi) controlled by software. FTIR-SEC experiments were performed using a cell acquired from LabOmak. This cell has two platinum grids as working and counter electrodes and an Ag wire as the pseudo-reference electrode. A N_2 saturated CH_3CN solution with 5 mM of **9** and 0.1 M of $TBAPF_6$ was injected in the FTIR-SEC cell. A linear voltammogram was performed using a scan rate of 10 mV s^{-1} to reach the desired reduction process. The IR spectra were obtained using a Nicolet Nexus 6700 FTIR spectrophotometer with a resolution of 4 $cm^{-1,}$ mirror velocity of 0.3165, aperture 32, gain 4 with 16 scans between 2200-1780 cm^{-1}. The background spectrum was performed with the sample at the open circuit potential.

X-Ray Data Collection. Crystals for single-crystal X-ray analysis of complexes **3**, **4**, **5**, **10**, and **11** were selected and covered with Fomblin (polyfluoro ether oil) and mounted on a nylon loop. The data were collected at 110K on a Bruker D8 Venture diffractometer equipped with a Photon 100 CMOS detector and an Oxford Cryosystem Cooler, using graphite monochromated Mo-Kα radiation (λ=0.71073 Å). The data was processed using the APEX3 suite software package, which includes integration and scaling (SAINT), absorption corrections (SADABS[40]) and space group determination (XPREP). Structure solution and refinement were done using direct methods with the programs SHELXT 2014/5 and SHELXL (version 2018/3)[41] inbuilt in APEX, SIR2019[42] and WinGX-Version 2020.1[43] software packages. In the crystal structure of **4**, a certain extent of disorder is observed, with 80% and 20% occupancy. All non-hydrogen atoms were refined anisotropically. Hydrogen atoms were inserted in idealized positions and allowed to refine riding on the parent carbon or oxygen atom with C–H distances of 0.95 Å, 0.98 Å, 0.99 Å, and 1.00 Å for aromatic, methyl, methylene and methine H atoms, respectively. The molecular diagrams were drawn with ORTEP-3 (version 2020.1),[44,45] included in the software package. Crystal and structure refinement data are given in Table S9. The data were deposited in the CCDC under deposit numbers 2060440 for **3**, 2060441 for **4**, 2060442 for **5** and 2060443 for **10**, and 2060444 for **11**.

Computational Details. All calculations were performed using the GAUSSIAN 09 software package[46] and the PBE0 functional without symmetry constraints. That functional uses a hybrid generalized gradient approximation (GGA), including 25 % mixture of Hartree-Fock[47] exchange with DFT[48] exchange-correlation, given by Perdew, Burke and Ernzerhof functional (PBE).[49-51] The basis set used consisted of the Stuttgart/Dresden ECP (SDD) basis set[52-54] with a *f*-polarization function[55] added to describe the electrons of manganese and the same basis set with a *d*-polarization function[56] added for bromine; the remaining elements were described by a standard 6-31G(d,p) basis set.[57-61] Frequency calculations were performed on the optimized geometries showing no imaginary modes and confirming the stationary points as minima. Solvent effects (acetonitrile) were considered in *all* calculations (geometry optimizations included) using the Polarizable Continuum Model (PCM) initially devised by Tomasi and coworkers[62-65] with radii and non-electrostatic terms of the SMD solvation model, developed by Truhlar *et al*.[66]

The values presented for the CO stretching frequencies are affected by a 0.955 scale factor. That factor results from the ratio between the experimental value for the highest ν(CO) of [$Mn(CO)_3$(bis-NHC^{Et})Br] (**9**), 1999 cm^{-1}, and the calculated one: 2094 cm^{-1}.

Conflicts of interest

There are no conflicts to declare.

Acknowledgements

We are grateful to Fundação da Ciência e a Tecnologia, FCT, for Projects PTDC/QUI-QIN/28151/2017, Project MOSTMICRO-ITQB UIDB/04612/2020, and UIPD/04612/2020 and the Swiss National Science Foundation (200021_182663) for financial support of this work. The NMR spectrometers at CERMAX through project 022162, and C. Almeida for HR-MS and elemental analysis at ITQB laboratories. S.R. and S.F. thank FCT for contract PTDC/QUI-QIN/28151/2017 and grant SFRH/BD/131955/2017, respectively. C.S.B. Gomes acknowledges LAQV and UCIBIO (UIDB/50006/2020, UIDP/50006/2020, UIDB/04378/2020, UIDP/04378/2020). Centro de Química Estrutural acknowledges the financial support of FCT (UIDB/00100/2020).

Notes and references

1 P. Mathew, A. Neels and M. Albrecht, *J. Am. Chem. Soc.*, 2008, **130**, 13534–13535.
2 G. Guisado-Barrios, J. Bouffard, B. Donnadieu and G. Bertrand, *Angew. Chem. Int. Ed.*, 2010, **49**, 4759–4762.
3 Á. Vivancos, C. Segarra and M. Albrecht, *Chem. Rev.*, 2018, **118**, 9493–9586.
4 K. F. Donnelly, A. Petronilho and M. Albrecht, *Chem. Commun.*, 2013, **49**, 1145–1159.
5 R. H. Crabtree, *Coord. Chem. Rev.*, 2013, **257**, 755–766.
6 B. Sarkar and L. Suntrup, *Angew. Chem. Int. Ed.*, 2017, **56**, 8938–8940.
7 P. Chábera, Y. Liu, O. Prakash, E. Thyrhaug , A. E. Nahhas, A. Honarfar, S. Essén, L. A. Fredin, T. C. B. Harlang, K. S. Kjær, K. Handrup, F. Ericson, H. Tatsuno, K. Morgan, J. Schnadt, L. Häggström, T. Ericsson , A. Sobkowiak, S. Lidin, P. Huang, S. Styring, J. Uhlig, J. Bendix, R. Lomoth, V. Sundström, and K. Wärnmark, *Nature*, 2017, **543**, 695-699.
8 D. Schweinfurth, L. Hettmanczyk, L. Suntrup and B. Sarkar, *Zeitschrift fur Anorg. und Allg. Chemie*, 2017, **643**, 554–584.
9 J. F. Schlagintweit, C. H. G. Jakob, K. Meigen-Berger, T. F. Gronauer, A. Weigert Muñoz, V. Weiß, M. Feige, S. A. Sieber, J. D. G. Correia and F. E. Kühn, *Dalton Trans.*, 2021, DOI:10.1039/d0dt04114a.
10 F. Al-Shnani, G. Guisado-Barrios, D. Sainz and E. Peris, *Organometallics*, 2019, **38**, 697–701.
11 C. Mejuto, B. Royo, G. Guisado-Barrios and E. Peris, *Beilstein J. Org. Chem.*, 2015, **11**, 2584–2590.
12 M. Van Der Meer, E. Glais, I. Siewert and B. Sarkar, *Angew. Chem. Int. Ed.*, 2015, **54**, 13792–13795.

13 H. Iwasaki, Y. Yamada, R. Ishikawa, Y. Koga and K. Matsubara, *Eur. J. Org. Chem.*, 2016, **2016**, 1651–1654.
14 C. Johnson and M. Albrecht, *Organometallics*, 2017, **36**, 2902–2913.
15 Y. Wei, S. X. Liu, H. Mueller-Bunz and M. Albrecht, *ACS Catal.*, 2016, **6**, 8192-8200.
16 S. G. Mncube and M. D. Bala, *Mol. Catal.*, 2020, **482**, 100107-100115.
17 A. Petronilho, H. Müller-Bunz and M. Albrecht, *Chem. Commun.*, 2012, **48**, 6499–6501.
18 H. Iwasaki, Y. Teshima, Y. Yamada, R. Ishikawa, Y. Koga and K. Matsubara, *Dalton Trans.*, 2016, **45**, 5713–5719.
19 C. Romain, S. Bellemin-Laponnza and S. Dagorne, *Coord. Chem. Rev.* 2020, **422**, 213411-213442.
20 W.-T. Lee, D. A. Dickie, A. J. Metta-Magaña and J. M. Smith, *Inorg. Chem*. 2013, **52**, 12842-12846.
21 M. F. Pinto, M. Olivares, Á. Vivancos, G. Guisado-Barrios, M. Albrecht and B. Royo, *Catal. Sci. Technol.*, 2019, **9**, 2421–2425.
22 F. Franco, M. F. Pinto, B. Royo and J. Lloret-Fillol, *Angew. Chem. Int. Ed.*, 2018, **57**, 4603-4606.
23 M. Pinto, S. Friães, F. Franco, J. Lloret-Fillol and B. Royo, *ChemCatChem* 2018, **10**, 2734-2740.
24 S. C. A. Sousa, C. J. Carrasco, M. F. Pinto and B. Royo, *ChemCatChem*, 2019, **11**, 3839–3843.
25 S. C. A. Sousa, S. Realista and B. Royo, *Adv. Synth. Catal.*, 2020, 1–8.
26 J. M. S. Cardoso, A. Fernandes, B. D. P. Cardoso, M. D. Carvalho, L. P. Ferreira, M. J. Calhorda and B. Royo, *Organometallics*, 2014, **33**, 5670-5677.
27 J. M. S. Cardoso and B. Royo, *Chem. Commun.*, 2012, **48**, 4944-4946.
28 J. M. S. Cardoso, R. Lopes and B. Royo, *J. Organomet. Chem.*, 2015 , **775**, 173-177.
29 S. Warratz, L. Postigo and B. Royo, *Organometallics*, 2013, **32**, 893-897.
30 S. Pottabathula and B. Royo, *Tetrahedron Lett.*, 2012, **53**, 5156-5158.
31 R. Lopes, J. M. S. Cardoso, L. Postigo and B. Royo, *Catal. Letters*, 2013, **143**, 1061–1066.
32 V. V. K. M. Kandepi, J. M. S. Cardoso, E. Peris and B. Royo, *Organometallics*, 2010, **29**, 2777–2782.
33 M. F. Pinto, B. D. P. Cardoso, S. Barroso, A. M. Martins and B. Royo, *Dalton Trans*., 2016, **45**, 13541-13546.
34 S. Bertini and M. Albrecht, *Organometallics*, 2020, **39**, 3413–3424.
35 Á. Vivancos and M. Albrecht, *Organometallics*, 2017, **36**, 1580–1590.
36 G. Guisado-Barrios, J. Bouffard, B. Donnadieu and G. Bertrand, *Organometallics*, 2011, **30**, 6017–6021.
37 L. H. Staal, A. Oskam and K. Vrieze, *J. Organomet. Chem*. 1979, **170**, 235-245.
38 V. Blase, T. Pape and F. E. Hahn, *J. Organomet. Chem.*, 2011, **696**, 3337–3342.
39 Single crystals of $[Mn_2(CO)_8(PPh_3)_2]$ were isolated from the mixture and studied by X-ray diffraction. Y. Zhao, H. W. Schmalle and H. Berke, *CSD Communication* 2016.
40 SADABS 2016/2: Krause, L.; Herbst-Irmer, R.; Sheldrick, G. M.; Stalke, D. *J. Appl. Cryst.* 2015, **48**, 3-10.
41 SHELXL: G. M Sheldrick, *Acta Crystallogr., Sect. C-Struct. Chem.* 2015, **71**, 3-8
42 C. B. Hübschle, G. M. Sheldrick and B. Dittrich, *J. Appl. Crystallogr.* 2011, **44**, 1281-1284.
43 M. C. Burla, R. Caliandro, B. Carrozzini, G. L. Cascarano, C. Cuocci, C. Giacovazzo, M. Mallamo, A. Mazzone and G. Polidori, *J. Appl. Cryst.* 2015, **48**, 306–309.
44 L. J. Farrugia, *J. Appl. Cryst.* 2012, **45**, 849-854.
45 C. R. Groom, I. J. Bruno, M. P. Lightfoot and S. C. Ward, *Acta Cryst.* 2016, ***B72***, 171-179.
46 Gaussian 09, Revision A.01, M. J. Frisch, G. W. Trucks, H. B. Schlegel, G. E. Scuseria, M. A. Robb, J. R. Cheeseman, G. Scalmani, V. Barone, B. Mennucci, G. A. Petersson, H. Nakatsuji, M. Caricato, X. Li, H. P. Hratchian, A. F. Izmaylov, J. Bloino, G. Zheng, J. L. Sonnenberg, M. Hada, M. Ehara, K. Toyota, R. Fukuda, J. Hasegawa, M. Ishida, T. Nakajima, Y. Honda, O. Kitao, H. Nakai, T. Vreven, Jr. J. A. Montgomery, J. E. Peralta, F. Ogliaro, M. Bearpark, J. J. Heyd, E. Brothers, K. N. Kudin, V. N. Staroverov, R. Kobayashi, J. Normand, K. Raghavachari, A. Rendell, J. C. Burant, S. S. Iyengar, J. Tomasi, M. Cossi, N. Rega, J. M. Millam, M. Klene, J. E. Knox, J. B. Cross, V. Bakken, C. Adamo, J. Jaramillo, R. Gomperts, R. E. Stratmann, O. Yazyev, A. J. Austin, R. Cammi, C. Pomelli, J. W. Ochterski, R. L. Martin, K. Morokuma, V. G. Zakrzewski, G. A. Voth, P. Salvador, J. J. Dannenberg, S. Dapprich, A. D. Daniels, Ö. Farkas, J. B. Foresman, J. V. Ortiz, J. Cioslowski and D. J. Fox, Gaussian, Inc., Wallingford CT, 2009.
47 W. J. Hehre, L. Radom, P. v. R. Schleyer & J. A. Pople, *Ab Initio Molecular Orbital Theory*, John Wiley & Sons, NY, (1986).
48 R. G. Parr and W. Yang, Density Functional Theory of Atoms and Molecules; Oxford University Press, New York, 1989. Values obtained at the PBE0-D3/6-311++G**//PBE0/b1 level.
49 J. P. Perdew, K. Burke and M. Ernzerhof, *Phys. Rev. Lett.* 1996, **77**, 3865-3868;
50 J. P. Perdew, K. Burke and M. Ernzerhof, *Phys. Rev. Lett.* 1997, **78**, 1396-1396.
51 J. P. Perdew, *Phys. Rev. B* **1986**, *33*, 8822-8824.
52 U. Haeusermann, M. Dolg, H. Stoll, H. Preuss, P. Schwerdtfeger and R. M. Pitzer, *Mol. Phys.* 1993, **78**, 1211-1224.
53 W. Kuechle, M. Dolg, H. Stoll and H. Preuss, *J. Chem. Phys.* 1994, **100***,* 7535-7542.
54 T. Leininger, A. Nicklass, H. Stoll, M. Dolg and P. Schwerdtfeger, *J. Chem. Phys.* 1996, **105**, 1052-1059.
55 E. A. Whlers, M. Böhme, S. Dapprich, A. Gobbi, A. Höllwarth, V. Jonas, K. F. Köhler, R. Stegmann, A. Veldkamp and G. A. Frenking, *Phys. Lett.* 1993, **208**, 111-114.
56 A. Höllwarth, M. Böhme, S. Dapprich, A. W. Ehlers, A. Gobbi, V. Jonas, K. F. Köhler, R. Stegmann, A. Veldkamp, and G. Frenking, *Chem. Phys. Lett*. 1993, **208**, 237-240.
57 R. Ditchfield, W. J. Hehre and J. A. Pople, *J. Chem. Phys*. 1971, **54**, 724-728.
58 W. J. Hehre, R. Ditchfield and J. A. Pople, *J. Chem. Phys*. 1972, **56**, 2257-2261.
59 P. C. Hariharan and J. A. Pople, *Mol. Phys*. 1974, **27**, 209-214.
60 M. S. Gordon, *Chem. Phys. Lett*. 1980, **76**, 163-168.
61 P. C. Hariharan and J. A. Pople, *Chim. Acta* 1973, **28**, 213-222.
62 M. T. Cancès, B. Mennucci and J. J. Tomasi, *Chem. Phys.* 1997, **107**, 3032-3041.
63 M. Cossi, V. Barone, B. Mennucci and J. Tomasi, *Chem. Phys. Lett.* 1998, **286**, 253-260.
64 B. Mennucci, J. Tomasi, *J. Chem. Phys.* 1997, **106**, 5151-5158.
65 J. Tomasi, B. Mennucci and R. Cammi, *Chem. Rev.* 2005, **105**, 2999-3094.
66 A. V. Marenich, C. J. Cramer and D. G. Truhlar,. *J. Phys. Chem. B*, 2009, **113**, 6378-6396.